Materials Transactions, Vol. 49, No. 7 (2008) pp. 1675 to 1680

Design of Cascaded Oxide Thermoelectric Generator

Lihua Zhang[1,*], Tsuyoshi Tosho[2], Noriyuki Okinaka[2] and Tomohiro Akiyama[2]

[1]*Graduate School of Engineering, Hokkaido University, Sapporo 060-8628, Japan*
[2]*Center for Advanced Research of Energy Conversion Materials, Hokkaido University, Sapporo 060-8628, Japan*

This paper describes the design of two- and three-stage cascaded oxide thermoelectric generators (TEGs) for high-temperature heat recovery using reported data to optimize energy conversion efficiency. We used the general intermetallic compounds $Bi_2(Se,Te)_3$ and $(Bi,Sb)_2Te_3$ for the low-temperature stages and oxides of $TiO_{1.1}$, La-doped $SrTiO_3$, $Na_xCo_2O_4$, and Al-doped ZnO for the higher-temperature stages. A two-stage TEG with $TiO_{1.1}$ as the *p*-type material and La-doped $SrTiO_3$ as the *n*-type material was found to have the highest efficiency at heat-source temperatures below 852 K, while the three-stage TEG was slightly more efficient than the two-stage TEG for heat-source temperatures above 852 K. For the three-stage TEG, the optimal boundary temperature of the second and third stages was calculated to be 698 K; at this temperature, the maximum energy conversion efficiency, 13.5%, was obtained at a heat-source temperature of 1223 K. The results showed that the designed two- and three-stage cascaded oxide TEGs have high potential for heat recovery from high-temperature waste.
[doi:10.2320/matertrans.MRA2008085]

(Received March 5, 2008; Accepted April 21, 2008; Published June 11, 2008)

Keywords: *heat recovery, cascaded thermoelectric generator, oxide thermoelectric materials, energy conversion efficiency*

1. Introduction

Thermoelectric (TE) devices can directly convert thermal energy into electric energy and vice versa.[1)] They are attractive energy-conversion devices for use in refrigeration or electrical power generation, possessing many advantages such as high reliability, infrequent service requirements, simple maintenance requirements, and long life. Current research on TE devices is largely focused on the development of better TE materials and the associated manufacturing techniques, thus expanding the range of applications of TE devices.[2–5)] For example, TE generators (TEGs) have already been used in military, aerospace, and commercial products as application-specific power-generation devices. Suzuki *et al.*[6–8)] designed a three-dimensional helical system TEG that is very compact and can save space in large-scale power generation. Additionally, it is known that the TE properties of materials vary considerably with temperature; therefore, it is not desirable, or is even impossible, to use the same material over a wide temperature range. Consequently, a *segmented TEG*[9–11)] and *cascaded TEG*[12–15)] have also been developed for high-efficiency energy conversion. Among these different TEG designs, the cascaded TEG design has been heavily researched because of its simple structure and easy fabrication.

One of the most promising potential fields of application for cascaded TEGs is the energy recovery of high-temperature waste heat, which is a considerable component in many industries.[16)] A cascaded TEG for such high-temperature applications should have high heat and oxidation resistance to achieve stable performance. For this reason, TEGs with cascaded structures that use oxide materials are studied theoretically in this paper.

Since the discovery of high TE properties in layered sodium cobalt oxide materials,[17)] many kinds of oxides have been exploited for TE application, such as perovskite oxides,[18–20)] electron-doped ZnO, and calcium cobalt oxides.[21–23)] In all the polycrystalline oxides, *p*-type non-stoichiometric titanium oxide ($TiO_{1.1}$)[24)] has been reported to have the highest *ZT* value of 1.64 at 1073 K (where *ZT* is a dimensionless figure of merit). And the *ZT* value is higher than one in the temperature range from 773 K to 1223 K; therefore, it has great potential in high-temperature applications. However, there is no report on the TE applications of this material, and few studies on cascaded oxide TEGs focus on TEG design and conversion efficiency optimization. Therefore, the purpose of this paper is to design a cascaded TEG that uses the previously reported oxides, including $TiO_{1.1}$, to optimize the energy conversion efficiency for different heat-source temperatures. In this paper, two two-stage and one three-stage cascaded TEGs are designed, and their efficiencies are calculated and analyzed.

2. Module Design of Cascaded Oxide TEG

Generally, a cascaded TEG has only two or three stages, because product cost and heat loss increase with the total stage number. Figure 1 shows a schematic diagram of a general cascaded TEG module with a three-stage structure. From heat source to heat sink, different semiconductor

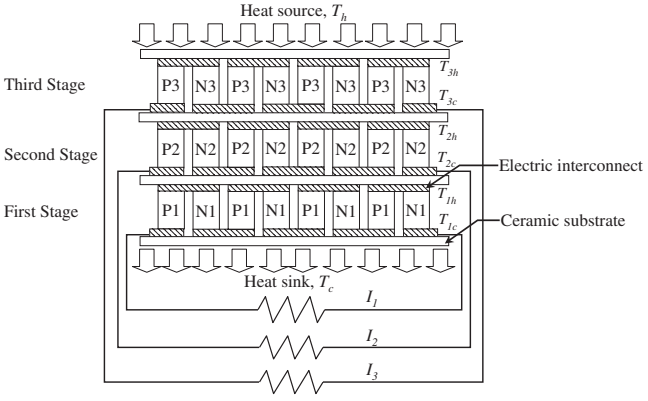

Fig. 1 Schematic diagram of a general cascaded TEG.

*Graduate Student, Hokkaido University

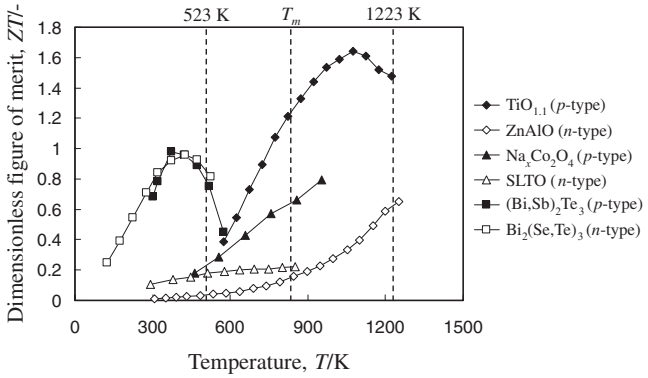

Fig. 2 Temperature dependence of the TE properties of the proposed materials, in which the oxides have the highest reported *ZT* values over 523 K.

materials are used as TE materials, and every stage has its own working temperature range. Heat is transferred from the heat source at T_h to the top stage of the cascaded TEG, then to the lower stages, and finally to the heat sink at T_c. The output electric currents I of each stage are different and independent, and the energy conversion efficiency of every stage can be optimized by the types of materials used and the dimensions.

Figure 2 shows the temperature dependence of the *ZT* value of the proposed materials for the cascaded oxide TEG in this paper. $TiO_{1.1}$, $Na_xCo_2O_4$, and $(Bi,Sb)_2Te_3$ are *p*-type semiconductors; Al-doped ZnO (henceforth denoted as ZnAlO), La-doped $SrTiO_3$ (henceforth, SLTO), and $Bi_2(Se,Te)_3$ are *n*-type. Table 1 lists the corresponding references for the data on selected oxide materials. These oxides were chosen for their comparatively more desirable properties and ease of fabrication in polycrystalline structures. Here, it should be mentioned that in Fig. 2, the *ZT* values for $TiO_{1.1}$ are the highest values obtained by our group;[24] and the highest reported *ZT* values for polycrystalline $Na_xCo_2O_4$ are used.[25] Additionally, we recently reported that polycrystalline SLTO prepared by combustion synthesis exhibits the highest *ZT* values;[18,19] therefore, these data were adopted in this paper. The intermetallic compounds $Bi_2(Se,Te)_3$ and $(Bi,Sb)_2Te_3$ are the TE materials that perform the best at low temperatures and have already been used in practical applications with lower production costs. The optimal working temperature of these intermetallic compounds is lower than 523 K; therefore, in this study, $Bi_2(Se,Te)_3$ and $(Bi,Sb)_2Te_3$ are used for the first stage of the proposed cascaded oxide TEG.

The combination of these materials can affect the energy conversion efficiency greatly; therefore, a proper combination of these materials is very important. As shown in Fig. 2, among *p*-type materials, $TiO_{1.1}$ has very desirable TE properties through a large temperature range and it can be used for both the second and third stages of a cascaded TEG. Among *n*-type materials, the *ZT* value of SLTO is higher than that of ZnAlO below 852 K; however, the temperature range of the available data for SLTO is only from room temperature to 852 K: this limitation is taken into consideration in the design. Figure 3 shows a schematic of the desired TEG. For the two-stage structure (Fig. 3(a)), $TiO_{1.1}$ serves as the *p*-type material in the second stage, while both ZnAlO and SLTO are candidates for use as *n*-type materials. For the three-stage structure (Fig. 3(b)), the second stage uses $Na_xCo_2O_4$ and SLTO; and the third stage, $TiO_{1.1}$ and ZnAlO.

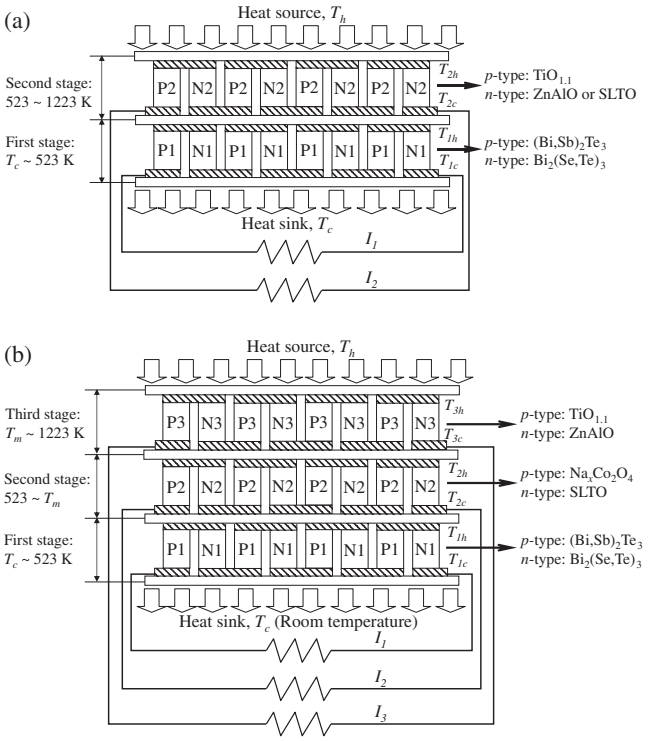

Fig. 3 Schematic diagrams of the proposed cascaded oxide TEG: (a) two-stage cascaded oxide TEG, (b) three-stage cascaded oxide TEG.

The energy conversion efficiency of the TE module can be calculated from the available data on these materials. To simplify the calculation, the junctions of the stages are assumed to be isothermal and to have negligible resistances to heat and electricity flow compared with the resistances of the n and p legs.

For one pair of TE semiconductors, the figure of merit Z is usually calculated using the following equation

Table 1 Selected candidate oxides for desired oxide TEG.

Temperature zone	Type	Candidate	Reference (Year)
Intermediate	*p*	$Na_xCo_2O_4$	Ito M., *et al.*[25] (2003)
	n	$Sr_{0.92}La_{0.08}TiO_3$ (SLTO)	Zhang L., *et al.*[18] (2007)
	n	$Zn_{0.98}Al_{0.02}O$ (ZnAlO)	Ohtaki M., *et al.*[23] (2006)
High	*p*	$TiO_{1.1}$	Okinaka N., *et al.*[24] (2006)
	n	$Zn_{0.98}Al_{0.02}O$ (ZnAlO)	Ohtaki M., *et al.*[23] (2006)

$$Z_{\mathrm{pn}} = \left[\frac{\langle \alpha_{\mathrm{p}} \rangle - \langle \alpha_{\mathrm{n}} \rangle}{\sqrt{\langle \kappa_{\mathrm{p}} \rangle \langle \rho_{\mathrm{p}} \rangle} + \sqrt{\langle \kappa_{\mathrm{n}} \rangle \langle \rho_{\mathrm{n}} \rangle}} \right]^2. \quad (1)$$

Here, α, κ, and ρ are the Seebeck coefficient, thermal conductivity, and electric resistivity, respectively; the subscripts n and p refer to the n-type and p-type TE materials, respectively. The electric conductivity σ is also usually used in the calculation of Z_{pn}, which is the reciprocal of ρ. Because α, κ, and ρ vary with temperature, the algebraic averages are generally used to simply calculation; however, the resulting error can be very large in some cases. In this paper, $\langle \alpha \rangle$, $\langle \kappa \rangle$, and $\langle \rho \rangle$ are used; they are defined as

$$\langle \alpha \rangle = \frac{1}{(T_2 - T_1)} \int_{T_1}^{T_2} \alpha dT \quad (2)$$

$$\langle \rho \rangle = \frac{1}{(T_2 - T_1)} \int_{T_1}^{T_2} \rho dT \quad (3)$$

$$\langle \kappa \rangle = \frac{1}{(T_2 - T_1)} \int_{T_1}^{T_2} \kappa dT. \quad (4)$$

T_1 and T_2 are the cold- and hot-side temperatures of a TE pair, respectively. The error in the calculation using this method is approximately 6%,[26] which is very close to that made using the method of numerical solution of ordinary differential equations.

Then the maximum efficiency of a TE pair can be calculated by

$$\eta_{\max} = \frac{T_2 - T_1}{T_2} \cdot \frac{(1 + Z_{\mathrm{pn}} T_{\mathrm{M}})^{1/2} - 1}{(1 + Z_{\mathrm{pn}} T_{\mathrm{M}})^{1/2} - \dfrac{T_1}{T_2}} \quad (5)$$

where T_{M} is the average temperature of T_1 and T_2,

$$T_{\mathrm{M}} = \frac{T_1 + T_2}{2}. \quad (6)$$

For a multistage cascaded TEG, the total maximum efficiency is

$$\eta_{\mathrm{Total}} = 1 - \prod_{i=1}^{n} (1 - \eta_i) \quad (7)$$

where η_i is the efficiency of the i^{th} stage and n is the total number of stages.

In this study, the maximum efficiency of the first stage provided in the reference data for the commercial product was used and was taken to be constant in the calculation. All of the available data on the TE properties of $TiO_{1.1}$ were gathered at temperatures below 1223 K; therefore, the highest heat-source temperature was set to 1223 K. The maximum energy conversion efficiencies of the two- and three-stage TEGs were calculated accordingly.

3. Calculation Results and Discussion

3.1 Two-stage cascaded oxide TEG

Figure 3(a) shows the structure of the designed two-stage cascaded oxide TEG. The first stage uses the intermetallic compounds $Bi_2(Se,Te)_3$ and $(Bi,Sb)_2Te_3$, and the working temperature range used is from room temperature to 523 K to avoid the oxidation and deterioration of the compounds.[26] For the second stage, the working temperature of the TEG

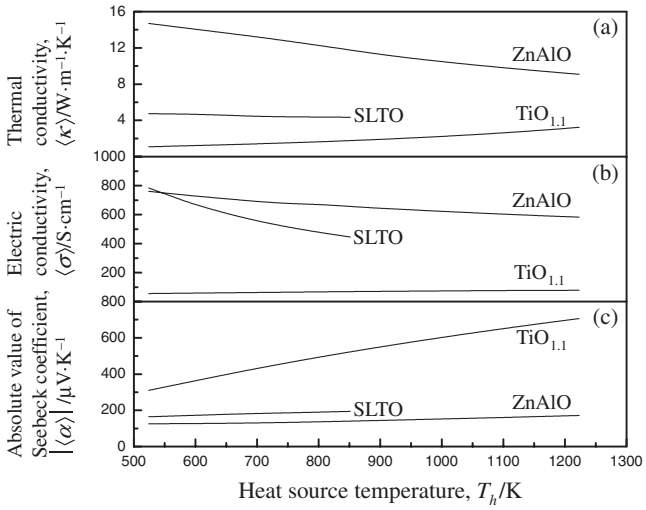

Fig. 4 Dependence on the heat-source temperature of the TE properties of the second-stage materials in two-stage TEG: (a) thermal conductivity, (b) electric conductivity, (c) absolute value of Seebeck coefficient.

can be as high as 852 K and 1223 K when the n-type materials are SLTO and ZnAlO, respectively. According to our assumptions, the following equations are obtained.

$$T_{1\mathrm{c}} = T_{\mathrm{c}} \quad (8)$$

$$T_{2\mathrm{c}} = T_{1\mathrm{h}} = 523K \quad (9)$$

$$T_{\mathrm{h}} = T_{2\mathrm{h}} \leq 1223K \quad (10)$$

In order to calculate the efficiency of the second stage, the temperature dependence of $\langle \alpha \rangle$, $\langle \kappa \rangle$, and $\langle \sigma \rangle$ on the hot side was calculated from the corresponding reported data by using eqs. (2)–(4). Figure 4 shows the dependence of the TE properties of $TiO_{1.1}$, SLTO, and ZnAlO on the heat-source temperature. Here it should be mentioned that the referenced data in this paper are scatter charts, and the line was calculated by interpolation; therefore, as shown in Fig. 4, the calculated results are drawn in lines.

Then the efficiency can be calculated by using eqs. (1), (5), and (7). For a two-stage TEG, equation (7) can be written as

$$\eta_{\mathrm{Total}} = 1 - (1 - \eta_1)(1 - \eta_2). \quad (11)$$

The calculation results are shown in Fig. 5. Throughout the heat-source temperature range, the efficiency increased with heat-source temperature; this was mainly caused by the increase in the Carnot efficiency of the second stage. Comparing the two-stage cascaded TEGs with different n-type materials, the TEG that uses SLTO as the n-type material has a higher maximum efficiency at heat-source temperatures below 852 K than does that which uses ZnAlO as the n-type material. The maximum efficiency of the TEG that uses SLTO was 9.1% at a heat-source temperature of 852 K; and the efficiency has an increasing potential at higher temperature. Ohta *et al.*[27] reported the TE properties of single-crystal SLTOs up to 1073 K and showed that the ZT increased with temperature up to 1073 K; however, the TE properties of SLTO at higher temperatures are not available. Therefore, the TE properties of polycrystalline SLTO need to be evaluated at high temperatures in the future. For the TEG that uses ZnAlO, the highest maximum efficiency, 13.2%, was obtained at 1223 K. The results show

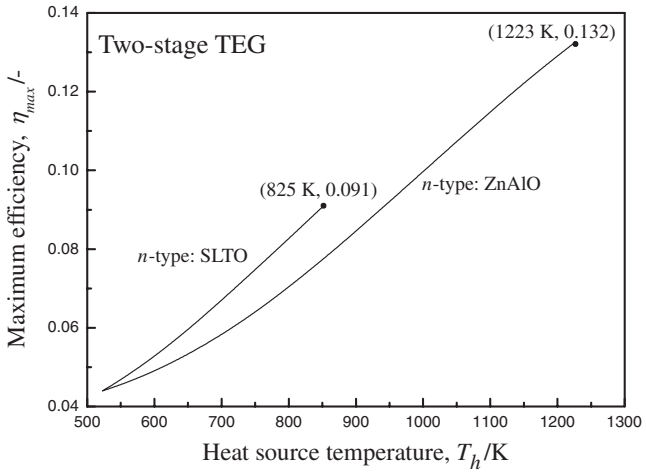

Fig. 5 Dependence on the heat-source temperature of the total maximum efficiency of the two-stage TEG with different *n*-type materials.

that at temperatures below 852 K, for the two-stage TEG, SLTO should be used as the *n*-type material. At present, ZnAlO is recommended as the *n*-type material for high temperature.

3.2 Three-stage cascaded oxide TEG

Figure 3(b) shows a schematic of the designed three-stage TEG. The first stage is the same as that of the two-stage TEG. Considering the working temperature range of each material, the second stage uses $Na_xCo_2O_4$ and SLTO, and the third stage uses $TiO_{1.1}$ and ZnAlO. In the second and third stages

$$T_{2h} = T_{3c} = T_m \quad (12)$$

$$T_{3h} = T_h \leq 1223K. \quad (13)$$

For the second and third stages, the efficiency is greatly affected by the working temperature range; therefore, it is necessary to find an optimal boundary temperature T_m.

As mentioned before, the data we have reported on the TE properties of SLTO are for a temperature range below 852 K; therefore, the T_m should be in that temperature range, from 523 to 852 K. The dependence on the heat-source temperature of the maximum efficiency for different T_m values was calculated using eqs. (1)–(7). For a three-stage TEG, the total efficiency can be written as

$$\eta_{Total} = 1 - (1 - \eta_1)(1 - \eta_2)(1 - \eta_3). \quad (14)$$

Figure 6 shows the contour lines of the total maximum efficiency obtained from the calculation. The *x*-axis shows the T_m value; the *y*-axis, the heat-source temperature. The heat-source temperature should be above T_m; therefore, only above the line $T_h = T_m$ do the contour lines have meaning. As shown in Fig. 6, the efficiency increased with the heat-source temperature, and the optimal T_m was in the range from 650 K to 750 K. According to the calculation results, when the T_m was 698 K, the highest efficiency, 13.5%, was obtained at a heat-source temperature 1223 K.

3.3 Comparison and application of the two- and three-stage TEGs

Figure 7 compares the maximum efficiencies of the designed two- and three-stage TEGs. At the same heat-

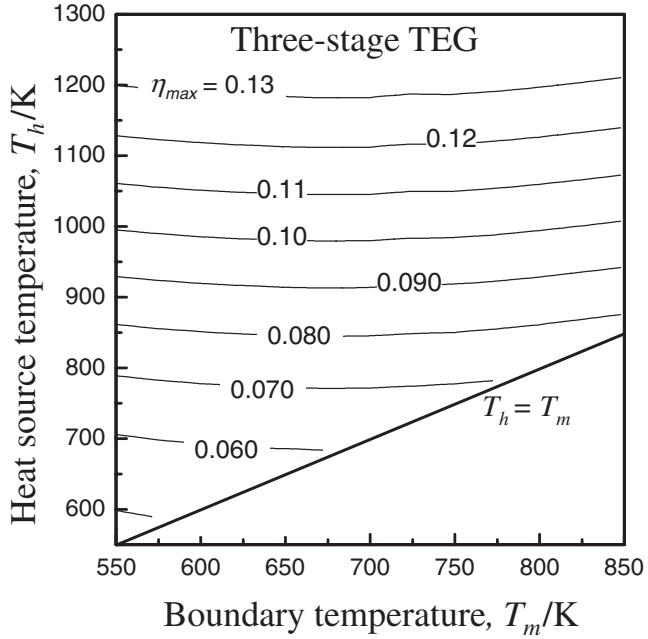

Fig. 6 Contour plot of the maximum energy conversion efficiency, η_{max}, on the graph of heat-source temperature, T_h, and boundary temperature, T_m.

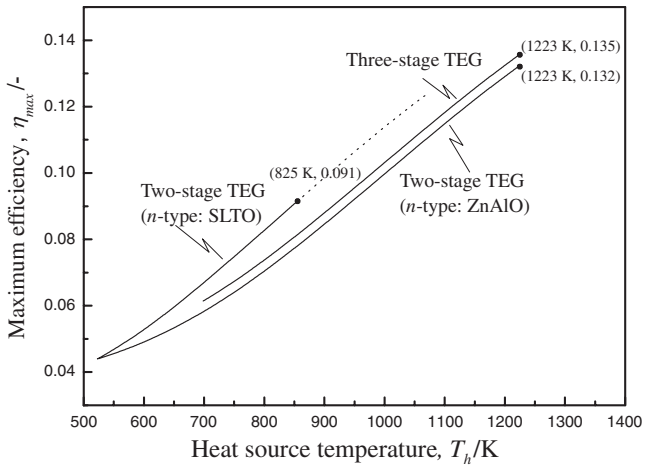

Fig. 7 Comparison of the maximum energy conversion efficiency of the two- and three-stage TEGs. (The dotted line represents data estimated using of the reported TE properties of the single-crystal SLTO.[27])

source temperature, the two-stage TEG that uses SLTO as the *n*-type material has the highest maximum efficiency when the heat-source temperature is below 852 K; the graph exhibits an upward trend for temperatures up to 1073 K, according to previous reports;[27] this previously reported data was represented by a dotted line and calculated from the data extrapolated from the TE properties we reported earlier.[18] At heat-source temperatures above 852 K, the three-stage TEG has higher maximum energy conversion efficiency than does the two-stage TEG that uses ZnAlO. Regarding energy conversion efficiency, the two-stage TEG that uses SLTO shows more potential for application in relatively low-temperature applications (from room temperature to 852 K); the three-stage TEG has a slightly higher

efficiency when the heat-source temperature is above 852 K. In practical applications of TEGs, the maximum efficiency will be lower than the calculated results because of the heat lost in between the stages. Furthermore, the two- and three-stage TEGs can be applied in different fields. For example, in waste heat recovery from water heating, drying industry, and low temperature curing industry, the two-stage TEG that uses SLTO as *n*-type material can be used; in industries with high-temperature steam generation, such as steelworks, the two-stage TEG that uses ZnAlO and three-stage TEG can be applied for waste heat recovery. As the energy conversion efficiencies of the two- and three-stage TEGs are very similar at high temperatures, in general, the two-stage TEG can be used extensively because of its relatively low production cost. Application of the three-stage TEG can be reserved for fields where the efficiency dominates the cost.

Although the energy conversion efficiency of our TEGs are at present lower than those of some other heat-recovery methods such as that of steam turbines, which is one of the most widely used in the generation of electricity from heat, the marked advantages of using oxide TEGs suggest a wide range of applications with great potential. We provide an example, assuming the three-stage TEG is applied in the Japanese steelworks industry to recover heat from molten slag, which is at about 1173 K. This is a cause of 273 MJ/ton-steel lost in waste heat. Assuming the annual Japanese steel yield is 1×10^8 ton, and assuming a maximum efficiency of 12.9% at 1173 K, 9.8×10^8 kWh can be generated every year, a not insignificant amount.

4. Conclusion

In this study, two- and three-stage cascaded TEGs were designed using state-of-the-art TE oxide materials in combination with the intermetallic compounds $Bi_2(Se,Te)_3$ and $(Bi,Sb)_2Te_3$, and the energy conversion efficiency was analyzed. The following results were obtained:

(1) At heat-source temperatures below 852 K, the maximum efficiency of the two-stage TEG that uses SLTO as the *n*-type material in the second stage is higher than that which uses ZnAlO. Regarding higher-temperature applications, the TEG that uses ZnAlO can obtain a maximum efficiency of 13.2% at 1223 K.

(2) For the desired three-stage TEG, when the boundary temperatures between the second and third stage is 698 K, the device can attain the highest efficiency; and the maximum efficiency of 13.5% is obtained when the heat-source temperature is 1223 K.

(3) Comparing the two- and three-stage TEGs, at heat-source temperatures below 852 K, the two-stage TEG that uses SLTO has the highest maximum efficiency; at higher temperatures, the maximum efficiency of the three-stage TEG is slightly higher than of the two-stage TEG that uses ZnAlO.

In conclusion, the two- and three-stage TEGs we designed showed high-energy conversion efficiencies in the TEG field, which indicates that cascaded oxide TEGs have great potential for applications in electricity generation from high-temperature waste heat.

Acknowledgements

The authors acknowledge the 21st Century COE Program "Topological Science and Technology" for partial financial support.

Appendix

I_i the current of generated electricity of the ith stage (A)
T_1 hot-side temperature of a TE pair (K)
T_2 cold-side temperature of a TE pair (K)
T_c heat-sink temperature (K)
T_h heat-source temperature (K)
T_{ic} cold-side temperature of the ith stage of a cascaded TEG (K)
T_{ih} hot-side temperature of the ith stage of a cascaded TEG (K)
T_M average temperature of the cold side and hot side of a TE pair (K)
T_m boundary temperature between the second and third stages in a three-stage TEG (K)
Z_{pn} figure of merit of a TE pair (K^{-1})

Greek symbols

α Seebeck coefficient of a general material ($\mu V \cdot K^{-1}$)
$\langle\alpha_n\rangle$ average Seebeck coefficient of *n*-type materials in the working temperature range ($\mu V \cdot K^{-1}$)
$\langle\alpha_p\rangle$ average Seebeck coefficient of *p*-type materials in the working temperature range ($\mu V \cdot K^{-1}$)
$\langle\alpha_{np}\rangle$ average Seebeck coefficient of a TE pair in the working temperature range ($\mu V \cdot K^{-1}$)
η_i energy conversion efficiency of the i^{th} stage (-)
η_{max} maximum energy conversion efficiency of the TEG (-)
η_{Total} the total energy conversion efficiency of the cascaded TEG (-)
$\langle\kappa_n\rangle$ average thermal conductivity of *n*-type materials in the working temperature range ($W \cdot m^{-1} \cdot K^{-1}$)
$\langle\kappa_p\rangle$ average thermal conductivity of *p*-type materials in the working temperature range ($W \cdot m^{-1} \cdot K^{-1}$)
$\langle\rho_n\rangle$ average electric resistivity of *n*-type materials in the working temperature range ($\Omega \cdot m$)
$\langle\rho_p\rangle$ average electric resistivity of *p*-type materials in the working temperature range ($\Omega \cdot m$)
σ electric conductivity of the material ($S \cdot m^{-1}$)

Subscripts

p *p*-type material
n *n*-type material

REFERENCES

1) D. M. Rowe: *Introduction*, (CRC Handbook of Thermoelectrics, Florida, CRC Press LLC, 1995) pp. 1–5.
2) P. X. Zhang, G. Y. Zhang, C. T. Lin and H. U. Habermeier: Egypt. J. Sol. **27** (2004) 1–7.
3) G. Min and D. M. Rowe: Energ. Convers. Manage. **43** (2002) 221–228.
4) K. Ono and R. O. Suzuki: J. Miner. Met. Mater. Soc. **50** (1998) 49–51.
5) F. J. Weinberg, D. M. Rowe and G. Min: J. Phys. D: Appl. Phys. **35** (2002) L61–L63.
6) R. O. Suzuki and D. Tanaka: J. Power. Sour. **122** (2003) 201–209.
7) R. O. Suzuki and D. Tanaka: J. Power. Sour. **132** (2004) 266–274.
8) R. O. Suzuki: J. Power. Sour. **133** (2004) 277–285.

9) T. Okamoto, S. Horii, T. Uchikoshi, T. S. Suzuki, Y. Sakka, R. Funahashi, N. Ando, M. Sakurai, J. Shimoyama and K. Kishio: Appl. Phys. Lett. **89** (2006) 081912.
10) T. Caillat, J.-P. Fleurial, G. J. Snyder, A. Zoltan, D. Zoltan and A. Borshchevsky: *Proc. 18th Int. Conf. Thermoelectrics*, ed. by A. Ehrlich, (Piscataway, NJ: IEEE, 1999) pp. 473–476.
11) G. J. Snyder and T. Caillat: MRS Proc. **793** (2004) 37.
12) L. Chen, L. Li, F. Sun and C. Wu: Appl. Energy. **82** (2005) 300–312.
13) J. Yu, H. Zhao and K. Xie: Cryogenics. **47** (2007) 89–93.
14) K. W. Lindler: Energy. Convers. Mgmt. **39** (1998) 1009–1014.
15) Y. Tanji, K. Kisara and M. Niino: Mater. Sci. Forum. **423–425** (2003) 813–818.
16) L. Zhang and T. Akiyama: Int. J. of Exergy. In press.
17) I. Terasaki, Y. Sasago and K. Uchinokura: Phys. Rev. B: Condens. Matter. **56** (1997) 12685–12687.
18) L. Zhang, T. Tosho, N. Okinaka and T. Akiyama: Mater. Trans. **48** (2007) 1079–1083.
19) L. Zhang, T. Tosho, N. Okinaka and T. Akiyama: Mater. Trans. **48** (2007) 2088–2093.
20) T. Okuda, K. Nakanishi, S. Miyasaka and Y. Tokura: Phys. Rev. B: Condens. Matter. **63** (2001) 113104.
21) T. Tsubota, M. Ohtaki, K. Eguchi and H. Arai: J. Mater. Chem. **85** (1997) 85–90.
22) M. Ohtaki, T. Tsubota, K. Eguchi and H. Arai: J. Appl. Phys. **79** (1996) 1.
23) M. Ohtaki and R. Hayashi: *Proc. 25th Int. Conf. Thermoelectrics*, (IEEE, Vienna, Austria, 2006) pp. 276–279.
24) N. Okinaka and T. Akiyama: Jpn. J. Appl. Phys. **45** (2006) 7009–7010.
25) M. Ito, T. Nagira, D. Furumoto and S. Katsuyama: Scri. Mater. **48** (2003) 403–408.
26) R. Sakata: *Handbook of Thermoelectrics-Principles and Applications*, (Realize Inc. Press, Tokyo, 2001) pp. 29–37.
27) S. Ohta, T. Nomura, H. Ohta and K. Koumoto: J. Appl. Phys. **97** (2005) 034106.